Numerical Evaluation of Key Performance of Railroad Concrete Crossties

Hailing Yu[1] and Daniel Mortarelli[2]

[1] John A. Volpe National Transportation Systems Center, Cambridge, MA 02142, USA

[2] Worcester Polytechnic Institute, Worcester, MA 01609, USA

Abstract: *In recent years, concrete rail ties have received additional scrutiny with respect to their design criteria, manufacturing processes, in track performance and failure modes, owing to a number of railway track deterioration/failure events resulting from premature concrete tie failure. This paper employs a finite element analysis (FEA) framework to examine the key performance of pretensioned concrete crossties, including the pretension-released surface strain profile/transfer length, splitting/bursting propensity due to prestress transfer, and flexural loading and displacement capacities in rail seat positive and center negative bending modes. The FEA framework employs the commercial FE software Abaqus and incorporates (1) a concrete damaged plasticity model capable of predicting concrete tensile cracking, and (2) a user defined elastoplastic bond model that characterizes the macroscopic interface behavior between various prestressing steel tendons and concrete. Two representative concrete tie designs, one with eight prestressing strands and the other with twenty prestressing wires embedded in the concrete, are considered in the numerical evaluations of their key performance defined above using the FEA framework. This study demonstrates that the FEA framework can be a cost-effective design tool to optimize the concrete crosstie performance against key industrial standard and track safety requirements.*

Keywords: *Pretensioned Concrete Crosstie, Prestress Transfer, Splitting Propensity, Rail Seat Positive Bending Performance, Center Negative Bending Performance, Performance Evaluation, Finite Element Analysis, Concrete Damaged Plasticity, Elastoplastic Bond Model*.

1. Introduction

With their first major installation in North America in 1966 (Hanna, 1979), concrete rail ties have been a promising alternative to timber ties, particularly in high speed and heavy haul applications. In recent years, interest has increased in examining the design criteria, manufacturing processes, in-track performance, and failure modes of pretensioned concrete crossties (e.g., Lutch, 2009b; Zeman, 2009; Yu, 2015a). Significant events that led to this additional scrutiny included, but were not limited to:

- Large scale occurrence of horizontal cracks and subsequent replacement of concrete ties on Amtrak’s Northeast Corridor (Mayville, 2014);

- Amtrak derailment accidents in Home Valley, WA (April 3, 2005) and Sprague, WA (January 28, 2006) due to rail seat abrasion damage in concrete ties (NTSB, 2006; Choros, 2007; Marquis, 2011);
- CSX freight train derailment on Metro-North's Hudson Division in Bronx, New York (July 18, 2013) resulting from center negative bending and bottom abrasion failures of concrete ties (NTSB, 2014; Marquis, 2014).

The Federal Railroad Administration (FRA) has sponsored extensive concrete tie research aimed at improving the safety performance of railroad concrete tie tracks and consequently reducing the derailment risks on these tracks. The research areas included prestress transfer and bonding qualities, characterization of track loading conditions, freeze-thaw performance and standards, flexural performance and standards, innovative materials, inspection technologies and computational methods. As a cost-effective research tool, the finite element analysis (FEA) method has increasingly complemented the laboratory and in-track testing approaches and contributed to achieving a better understanding of the concrete crosstie behaviors (e.g., Yu, 2011; Yu, 2012; Chen, 2014).

There are two key components in the material modeling of concrete crossties embedded with prestressing steel elements: a concrete material model capable of predicting concrete material failures (particularly tensile cracking), and a bond model capable of differentiating and realistically predicting the various concrete-steel reinforcement interface behaviors. An FEA framework—incorporating a concrete damaged plasticity model, which combines concrete damaged elasticity with tensile and compressive plasticity, and a user-defined, unified elastoplastic bond model—was previously developed and applied in several concrete crosstie studies, including predicting the concrete tie vertical deflection profiles under worn tie and/or deteriorated ballast support conditions (Yu, 2016a), evaluating the center negative flexural performance in derailment conditions (Yu, 2017a), and investigating the causes and preventive measures for splitting/bursting failures (Yu, 2017b and 2017c).

This paper applies the FEA framework in a comparative performance evaluation study for different concrete tie designs. While many concrete tie designs exist, including emerging post-tensioning designs, this paper focuses on two typical pretensioned concrete crosstie designs: one embedded with eight prestressing strands and the other with twenty prestressing wires. Further, the following set of metrics was selected for evaluating concrete tie performance using the FEA:

- Pretension-released surface strain profiles and transfer length calculations;
- Splitting/bursting propensity;
- Rail seat positive bending performance; and,
- Center negative bending performance.

Even though these metrics do not include all the performance issues discussed above, they cover critical concrete tie performance measures governing durability and safety. The performance metrics also conform to the type of solid mechanics problems that the FE method is capable of solving.

2. Finite element modeling approach

This section describes the two concrete tie designs under consideration, their FE models (mainly the concrete material and bond model parameters), and the detailed analysis methods. The commercial FE software Abaqus was employed (Dassault Systèmes Simulia Corp., 2012).

2.1 Concrete tie designs

Concrete tie design parameters can include: concrete mix design that determines concrete short- and long-term properties; reinforcement type (strand versus wire), diameter, number, spatial distribution, surface geometry and pretensioning force amount; non-prismatic geometric dimensions; and, steel versus concrete volumes. Two common concrete tie designs were considered for a comparative numerical study of their performance; they are hereafter identified as Tie A and Tie B.

As shown in Figure 1, Tie A (Yu, 2017a) has eight prestressing strands, each made with seven wires stranded together resulting in a nominal diameter of 3/8 inches (9.525 mm), and Tie B (Lutch, 2009a) has twenty prestressing wires, each with a nominal diameter of 0.209 inches (5.32 mm). Their main geometric dimensions and prestressing properties are summarized in Table 1. Both ties share the same length. Tie A is wider but has lower heights than Tie B. Overall both ties have comparable concrete volumes, but Tie A has a larger nominal steel volume.

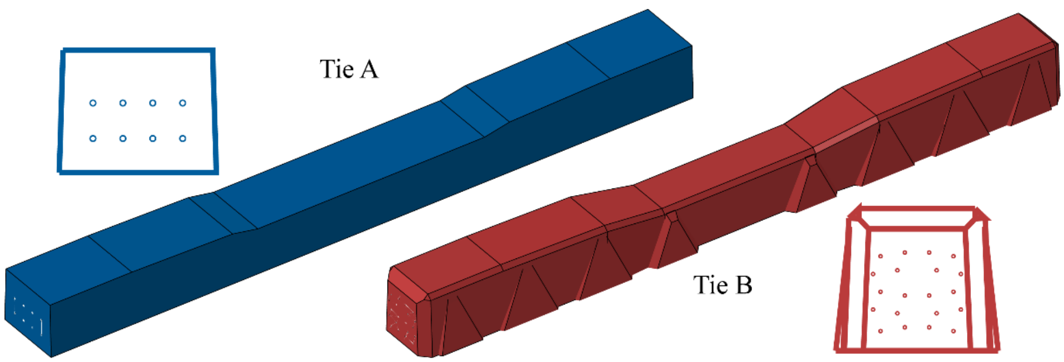

Figure 1. Schematic of concrete tie designs A and B.

Under the sponsorship of FRA, Kansas State University (KSU) conducted bond tests and transfer length measurements on fifteen prestressing wires and strands commercially available for manufacturing concrete crossties (e.g., Bodapati, 2013). The seven-wire strands (denoted as SA in the KSU project) used in making Tie A have natural spiral surfaces. For the wire reinforcements of Tie B, four variations in the wire surface geometry were considered in this study, corresponding to wires WA, WE, WG and WH identified in the KSU study (e.g., Bodapati, 2013). Of these four wires, WA was smooth, WE had spiral surface indentations, and WG and WH had chevron-shaped surface indentations. Wires WG and WH were further differentiated by their indentation dimensions. The different surface diameters/geometries of these four wires and the seven-wire strand yielded a range of bond-slip relations and transfer length properties for the concrete tie production (e.g., Arnold, 2013; Bodapati, 2013). Adding the reinforcement surface geometry variable in this study enabled a more thorough investigation of the effect of bond on concrete tie performance. As a result, there were effectively five tie designs considered in this study, namely, Tie A with 8 seven-wire strands, Tie B with 20 WA wires, Tie B with 20 WE wires, Tie B with 20 WG wires and Tie B with 20 WH wires.

Table 1. Comparison of concrete tie designs A and B.

	Tie A	**Tie B**
Dimension		
Length	102 in. (2,590.8 mm)	102 in. (2,590.8 mm)
Length of center section	36 in. (914.4 mm)	24 in. (609.6 mm)
Height of center section	7 in. (177.8 mm)	7.5 in. (190.5 mm)
Height at rail seat center	8 in. (203.2 mm)	9.29 in. (236.0 mm)
Base width at center	10.5 in. (266.7 mm)	8.37 in. (212.6 mm)
Base width at ends	10.5 in. (266.7 mm)	9.875 in. (250.8 mm)
Steel Reinforcement		
Type (number)	Seven-wire strand (8)	Single wire (20)
Nominal diameter	0.375 in. (9.525 mm)	0.209 in. (5.32 mm)
Pretension	156 ksi (1,075.6 MPa)	203 ksi (1,399.6 MPa)
Volume		
Steel reinforcement	90 in^3 (1,474.8 cm^3)	70 in^3 (1,147.1 cm^3)
Concrete	7,913 in^3 (129,670.8 cm^3)	7,919 in^3 (129,769.2 cm^3) (without scallops) 8,221 in^3 (134,718.1 cm^3) (with scallops)

2.2 Concrete tie models

The geometric modeling of the concrete and the steel tendons was straightforward following the respective tie designs (with the exception of the surface geometries, see “Interface Bond Model”). The steel tendons were modeled with linear elasticity followed by rigid-perfectly plasticity, but the stresses in the steel tendons were not expected to reach or exceed the yield strengths.

2.2.1 Concrete material

The concrete was modeled with a damaged plasticity model that used isotropic damaged elasticity in combination with isotropic tensile and compressive plasticity to represent the inelastic behavior of concrete (Dassault Systèmes Simulia Corp., 2012). With this material model, a tensile damage variable d_t was employed to measure the degree of tensile strength degradation, where d_t=0 indicated undamaged concrete, and d_t=1 indicated completely degraded tensile strength and formation of macro-cracks.

Concrete material properties evolve over time. Therefore, two sets of concrete material properties, at pretension release and long-term, were employed as shown in Table 2. The release properties corresponded to a nominal concrete release strength of 6,000 psi (41.4 MPa). The long-term properties were the same as those applied in a previous study (Yu, 2017a).

2.2.2 Interface bond model

The surface geometries of the steel reinforcements and concrete were homogenized, and the steel-concrete interface was represented with a thin layer of cohesive elements. Elastoplastic constitutive relations were developed in terms of normal and shear stresses versus interfacial dilatation and slip, and these phenomenological relations were assigned to the cohesive elements to reproduce the bond-slip and dilatational effects in the steel tendon-concrete interfaces. Previous work developed independent bond models and their FE implementations for the smooth wire WA (Yu, 2014), the seven-wire strand SA (Yu, 2015b) and the indented wires WE, WG and WH (Yu, 2016b). Most recently, unified elastoplastic formulations were developed and implemented to characterize the bond behaviors of the diversity of reinforcements described above using one bond model (Yu, 2018). Table 2 also shows the calibrated and validated bond model parameters for the five tendons corresponding to a nominal concrete release strength of 6,000 psi (41.4 MPa).

Table 2. Concrete material and interface bond model parameters.

Concrete material parameter		**Release**		**Long-term**	
Elastic modulus		4,028 ksi (27.8 GPa)		4,941.0 ksi (34.1 GPa)	
Poisson's ratio		0.200		0.202	
Split tensile strength		478.8 psi (3.3 MPa)		1,012.5 psi (6.98 MPa)	
Compressive strength		5,977.8 psi (41.2 MPa)		10,138.5 psi (69.9 MPa)	
Interface bond parameter	**Seven-wire strand SA**	**Smooth wire WA**	**Indented wire WE**	**Indented wire WG**	**Indented wire WH**
$D_{\mathrm{nn}}^{\mathrm{e}}$	92,630,000 lbf/in^3 (25,144.2 N/mm^3)	12,889,500 lbf/in^3 (3,498.8 N/mm^3)			
$D_{\mathrm{ns}}^{\mathrm{e}} (= D_{\mathrm{nt}}^{\mathrm{e}})$	385,958 lbf/in^3 (104.8 N/mm^3)	268,531 lbf/in^3 (72.9 N/mm^3)			
$\tan\phi$	0.30	0.45	0.50	0.40	0.65
a_0	600 psi (4.14 MPa)	253 psi (1.74 MPa)	550 psi (3.79 MPa)	400 psi (2.76 MPa)	1,000 psi (6.89 MPa)
$u_{\mathrm{tc}}^{\mathrm{pl}}$	0.08 in (2.03 mm)	0.077 in (1.96 mm)	0.120 in (3.05 mm)	0.067 in (1.70 mm)	0.050 in (1.27 mm)
$\mu_{\mathrm{d}}^{\max}$	0.0036	0.0000	0.0100	0.0145	0.0140
μ_{dc}	0.0036	0.0000	0.0050	0.0045	0.0045
$u_{\mathrm{td}}^{\mathrm{pl}}$	0.200 in (5.08 mm)	0.100 in (2.54 mm)	0.150 in (3.81 mm)	0.070 in (1.78 mm)	0.053 in (1.35 mm)

2.3 Analysis methods

The pretension release process was simulated by assigning pretensioning stresses in the steel tendons and then releasing the pretensions in a static FEA step. The resulting pretension-released stress states were then applied as initial conditions in subsequent static or dynamic FEA of the concrete ties subjected to laboratory or in-track loading conditions.

To obtain the pretension-released strain profile and evaluate the splitting/bursting propensity, the "release" concrete properties in Table 2 were applied. Ideally, the release properties applied to simulate pretension releases can be switched to long-term properties to simulate the usually late-age bending behaviors; however, the FEA program was inflexible with changing material properties between continued analyses, and therefore, the FEA conducted for evaluating the bending performance assumed long-term concrete properties throughout the analyses.

The scallops on the sides of Tie B were designed to enhance lateral stability. To minimize meshing difficulties, the scallop meshes were independently developed and then constrained to follow the movement of the main concrete tie mesh (Dassault Systèmes Simulia Corp., 2012). This setup sometimes led to premature non-convergence issues when simulating the bending behavior in the static FEA. FE simulations conducted in other research have shown insignificant differences in the bending behavior with or without the scallops. Therefore, the scallops were excluded in the static simulations of the flexural performance.

It is well known that concrete creep, concrete shrinkage and steel relaxation can lead to prestress losses in the steel reinforcements. Prestress losses were simulated as a worn tie condition in this paper by reducing the full pretension amounts in Table 1 by a predetermined prestress loss amount.

3. Results

As discussed in the introduction, four concrete tie performance measures, namely pretension-released surface strain profile and transfer length, splitting/bursting propensity, rail seat positive bending performance, and center negative bending performance, were included in the numerical study of the performance of Ties A and B, and the results are presented in this section.

3.1 Pretension-released surface strain profile and transfer length

For pretensioned concrete crosstie members, transfer lengths are defined as the distance needed to transfer the prestress from the steel reinforcements to the concrete, as measured from the end of a crosstie. Because rail loading is transmitted directly through the rail seat, a transfer length cannot be greater than the distance from the tie end to the rail seat. Transfer lengths have been used as an indicator of the prestress transfer quality in pretensioned concrete crosstie productions. It has been a common practice to measure the surface strain profiles upon pretension release and then use the strain data to calculate the transfer lengths.

Figure 2 shows the FEA predicted surface strain profiles in pretension-released concrete Ties A and B with the nominal concrete release strength of 6,000 psi (41.4 MPa). The Tie A results are shown for strand SA, and the Tie B results are shown for wires WA, WE, WG and WH. The strain profiles were clearly differentiated by the reinforcement types.

Figure 3 further shows the transfer length calculations based on the pretension-released strain profiles obtained from both the test data and the FEA simulations. It is noted that the test data included up to six sets of measurements made with Whittemore gauges; the FEA data included creep strain adjustments to the elastic strain profiles shown in Figure 2; and a statistically-based Zhao-Lee (or ZL) method, believed to yield unbiased and more accurate transfer length estimations than the 95 percent AMS method (Zhao, 2013), was employed to calculate the transfer lengths shown in Figure 3. The FEA predictions of the transfer length agreed well with the data obtained from the tests.

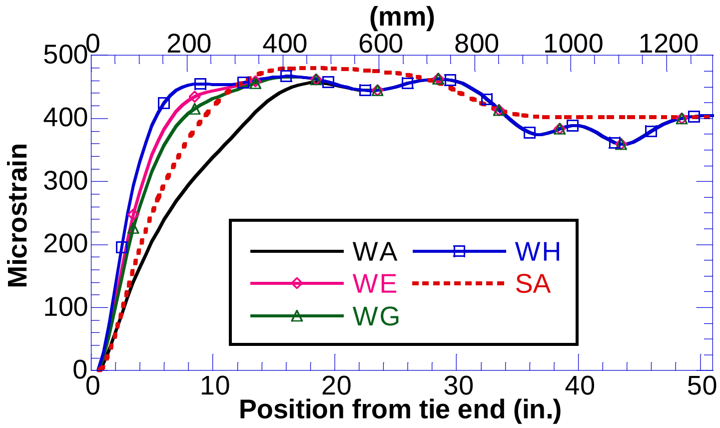

Figure 2. Surface strain profiles of concrete Ties A (made with strand SA) and B (made with wire WA, WE, WG or WH).

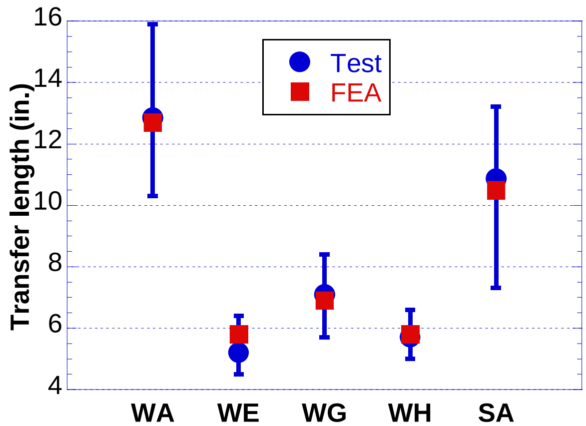

Figure 3. Transfer lengths for concrete Ties A (made with strand SA) and B (made with wire WA, WE, WG or WH): test (minimum, average and maximum) vs. FEA.

3.2 Splitting/bursting propensity

Horizontal splitting cracks were previously reported on a type of concrete tie made with two rows of prestressing strands (Mayville, 2014). For concrete ties made with prestressing wires, bursting cracks initiating and branching out from the steel tendon-concrete interfaces were more common. The appearances of splitting/bursting cracks can raise safety concerns and increase railroad maintenance demands.

The FEA has shown that the prestress transfer process during concrete tie production introduces tensile strength degradations to various degrees in the concrete surrounding the steel tendons. This initial damage can evolve with loading and environmental conditions, and develop into macroscopic splitting/bursting cracks.

Figure 4 shows the tensile damage variable (d_t) contours for Tie A upon pretension release at the 6,000 psi (41.4 MPa) concrete strength. The contour on the left was plotted for the entire quarter symmetric tie model, and it showed that the majority of the concrete did not experience instances of tensile damage (or tensile strength degradations). The contour on the right was plotted only for elements satisfying the condition $d_t > 0.001$, i.e., with nontrivial tensile damage. Quantitative indicators of splitting/bursting propensity can be extracted from this contour as follows: $d_{t,max}$ (the maximum d_t), deteriorated length l (maximum length measurement of the contour in the tie's length direction), deteriorated volume Vol (volume of elements included in the contour) and average deteriorated cross-sectional area (=Vol/l or $Vol÷l$).

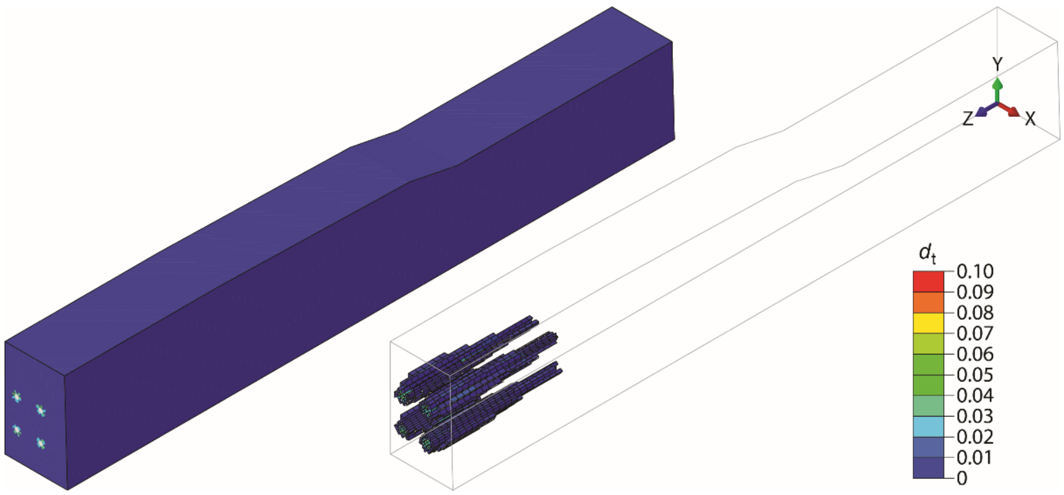

Figure 4. Tensile damage variable (d_t) contours for Tie A upon pretension release (quarter symmetric model is shown).

Table 3 summarizes the four splitting/bursting propensity indicators calculated based on the FEA of Ties A (with SA) and B (with WA, WE, WG or WH). As expected, although the smooth wire WA had the least favorable bond and prestress transfer properties, it was least susceptible to splitting/bursting failures. The strand SA appeared to have the worst splitting/bursting propensity. Further, the $d_{t,max}$ indicators suggested that the initial tensile damage was not significant for any of the five reinforcements with the 6,000 psi (41.4 MPa) concrete release strength.

3.3 Rail seat positive flexural performance

The American Railway Engineering and Maintenance-of-Way Association's (AREMA) Tie Manual specifies the performance of a rail tie in four bending modes (AREMA, 2010). With good ballast and subgrade support, a rail tie is expected to be in a rail seat positive bending mode. The AREMA rail seat positive moment test setup for monoblock concrete ties (AREMA, 2010) is reproduced in Figure 5 for a 102 inch (2.59 m) tie. The symbol for the applied vertical load was changed to "V" to distinguish from the load "P" applied in the center negative bending test (see section 3.4, "Center Negative Flexural Performance").

Table 3. Quantitative indicators of splitting/bursting propensity calculated on one full tie end.

Parameter	Tie A	Tie B			
	Seven-Wire Strand SA	**Smooth Wire WA**	**Indented Wire WE**	**Indented Wire WG**	**Indented Wire WH**
$d_{t,max}$	0.08	0.03	0.04	0.07	0.03
Deteriorated length *l* (d_t > 0.001)	11.08 in (28.2 cm)	11.26 in (28.6 cm)	7.41 in (18.8 cm)	7.96 in (20.2 cm)	6.86 in (17.4 cm)
Deteriorated volume *Vol* (d_t > 0.001)	78.7 in^3 (1289.4 cm^3)	18.5 in^3 (303.0 cm^3)	21.2 in^3 (347.7 cm^3)	33.9 in^3 (554.8 cm^3)	19.1 in^3 (312.9 cm^3)
Average deteriorated cross-sectional area (*Vol*÷*l*)	7.10 in^2 (45.8 cm^2)	1.64 in^2 (10.6 cm^2)	2.86 in^2 (18.5 cm^2)	4.25 in^2 (27.4 cm^2)	2.78 in^2 (18.0 cm^2)

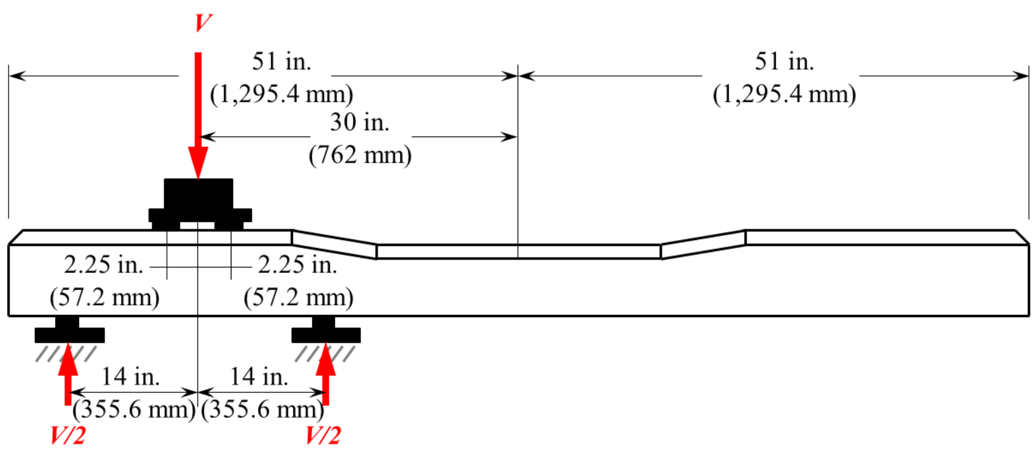

Figure 5. AREMA rail seat positive moment test specification for monoblock concrete ties (AREMA, 2010), reproduced for a 102 in. (2.59 m) tie.

The AREMA Tie Manual defines a "structural crack" as "a crack originating in the tensile face of the tie, extending to the outermost level of reinforcement or prestressing tendons and which increases in size under application of increasing load." In an AREMA rail seat positive moment test, a concrete tie is subjected to a load that produces a required rail seat positive moment, and the tie is considered to pass the test if there are no structural cracks observed with the applied load.

The FEA evaluation of the bending performance using the test in Figure 5 went further than the AREMA specification by loading the concrete ties to complete failure. The rail seat positive flexural performance was examined in terms of load and vertical displacement characteristics, with structural cracking and at complete failure. The results for all five ties are summarized in Table 4. The displacements were those of the rail seats relative to the supports under the tie. All ties showed small relative rail seat displacements when structural cracking or complete failure occurred. All displacement and load parameters were very comparable among the five ties, except that Tie B with wire WH had a higher load at complete failure than the other four ties. It is noted that static analyses were conducted to simulate the tests, and the static loads at complete failure depended on the convergence of the simulations, so the failure loads in Table 4 were lower bounds of actual failure loads that can be achieved.

Table 4. Rail seat positive flexural performance parameters.

Parameter	Tie A	Tie B			
	Seven-wire strand SA	**Smooth wire WA**	**Indented wire WE**	**Indented wire WG**	**Indented wire WH**
Static load with structural cracking	78.2 kip (348.1 kN)	82.4 kip (366.4 kN)	82.1 kip (365.2 kN)	83.5 kip (371.4 kN)	82.5 kip (367.0 kN)
Displacement with structural cracking	0.03 in (0.76 mm)	0.03 in (0.89 mm)	0.03 in (0.89 mm)	0.04 in (0.91 mm)	0.04 in (0.90 mm)
Static load at complete failure	96.6 kip (429.7 kN)	91.2 kip (405.8 kN)	90.8 kip (404.1 kN)	95.9 kip (426.8 kN)	110.6 kip (491.9 kN)
Displacement at complete failure	0.05 in (1.27 mm)	0.04 in (1.05 mm)	0.04 in (1.05 mm)	0.05 in (1.16 mm)	0.06 in (1.48 mm)

3.4 Center negative flexural performance

The AREMA center negative moment test (AREMA, 2010) is designed to evaluate the tie flexural performance under a deteriorated ballast support condition. The July 18, 2013 CSX freight train derailment on the Metro-North tracks was believed to be caused by complete failures of multiple, consecutive concrete ties in track in the center negative bending mode (Marquis, 2014; Yu, 2017a). In a study of the center negative bending performance of Tie A, which was the design of the concrete ties that made up the tracks at the derailment site, it was argued that the AREMA center negative bending test setup may not accurately reflect the actual field conditions, and a hypothetical deteriorated ballast support condition shown in Figure 6 was applied instead (Yu, 2017a). This deteriorated ballast support condition featured uneven gaps along the tie-ballast interfaces, and it was believed to be the likely field condition that caused the concrete tie center negative bending failures which in turn contributed to the derailment.

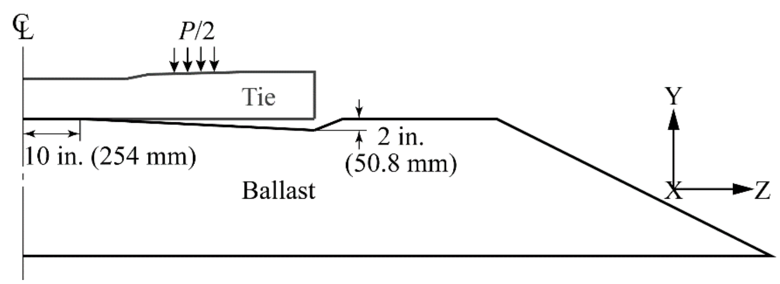

Figure 6. Concrete tie in a hypothetical center negative bending condition due to deteriorated ballast support, depicted in a half symmetric lengthwise plane (Yu, 2017a).

Dynamic FEA was conducted first for the ballast condition in Figure 6 for all five ties in the "no worn" condition, assigning full pretensions (see Table 1) and maintaining full cross sections (see Figure 1) of the ties. The load *P* was increased by increments of 1 kip (4.45 kN) in the simulations. At smaller *P*'s, the tie may show damage but not complete failure, the latter defined as the state of completely losing the load carry capability. The load *P* in the first simulation to show complete tie failure was accepted as a dynamic failure load. The maximum vertical relative rail seat displacement (VRRSD) with reference to the tie center and reached at the prior load level (1 kip lower than the failure load) was considered to be the maximum rail seat displacement capacity. The dynamic load and VRRSD causing structural cracking were also recorded.

The center negative bending performance parameters described above for all five ties are summarized in Table 5 under "No Worn Condition." It was observed that the load performance among all five ties and the VRRSD performance among the four Tie B variations were very consistent, indicating that the wire surface geometry did not differentiate the bending performance. Further, Tie A was shown to have a larger displacement capacity than Tie B, likely owing to the tie's reinforcement configurations as well as geometric dimensions.

Table 5. Center negative flexural performance parameters of concrete ties in "no worn" conditions.

Parameter (No Worn Condition)	Tie A	Tie B			
	Seven-Wire Strand SA	**Smooth Wire WA**	**Indented Wire WE**	**Indented Wire WG**	**Indented Wire WH**
Dynamic load with structural cracking	32.0 kip (142.3 kN)	31.0 kip (138.0 kN)	31.9 kip (141.8 kN)	31.9 kip (141.8 kN)	31.8 kip (141.2 kN)
VRRSD with structural cracking	0.15 in (3.7 mm)	0.10 in (2.4 mm)	0.10 in (2.5 mm)	0.10 in (2.5 mm)	0.10 in (2.5 mm)
Dynamic load at complete failure	41 kip (182.4 kN)	43 kip (191.3 kN)	43 kip (191.3 kN)	43 kip (191.3 kN)	44 kip (195.7 kN)
VRRSD prior to complete failure	0.40 in (10.2 mm)	0.29 in (7.4 mm)	0.28 in (7.2 mm)	0.29 in (7.3 mm)	0.31 in (7.9 mm)

Dynamic FEA were further conducted for the ballast condition in Figure 6 for Tie A (made with strand SA) and Tie B (made with wire WH) in worn conditions. Two worn concrete tie conditions—prestress loss and reduced cross sections due to bottom abrasion—were considered in the previous derailment study (Yu, 2017a). Prestress losses can occur to never-used and heavily-used concrete ties alike, whereas concrete tie bottom abrasion has shown to result from extended tie-ballast interactions under repeated track loading. The two worn concrete tie conditions were defined herein as:

1. Prestress loss in the amount of 40 ksi (310.3 MPa), translated to 116 ksi (799.8 MPa) pretension in SA and 163 ksi (1,123.8 MPa) pretension in WH in the simulations.
2. Loss of 1 inch (25.4 mm) deep of concrete materials from the tie bottom across the entire tie length.

The 40 ksi (310.3 MPa) prestress loss was the estimated life-time prestress loss in stress relieved steel strands (Naaman, 2012).

The FEA results of the center negative bending performance of Tie A and Tie B (made with wire WH) in worn conditions are also summarized in Table 6. The Worn Condition 1 (i.e., prestress loss) was applied to both ties, and the combined Worn Conditions 1 and 2 (i.e., prestress loss and bottom abrasion) were further applied to Tie A. The results indicated that the prestress losses decreased the failure loads but increased the displacements that the ties can tolerate prior to failure, and this effect was more prominent in the Tie A design than in the Tie B design. When the prestress loss condition was coupled with bottom abrasion in the Tie A analyses, the maximum load that the tie can sustain without failure was significantly reduced, indicating vastly increased risks of an unsafe track with broken ties. (The Worn Condition 2 was applied unsuccessfully to the pretension release simulation of Tie B, as it left too small a concrete cover for the bottom prestressing wires and constituted an unstable and insolvable numerical condition.)

Table 6. Center negative flexural performance parameters of concrete ties in worn conditions.

Parameter (Worn Conditions)	Tie A (Strand SA)		Tie B (Wire WH)
	Worn Condition 1	Worn Conditions 1&2	Worn Condition 1
Dynamic load with structural cracking	25.9 kip (115.3 kN)	19.0 kip (84.6 kN)	26.4 kip (117.5 kN)
VRRSD with structural cracking	0.12 in (3.0 mm)	0.15 in (3.8 mm)	0.08 in (2.0 mm)
Dynamic load at complete failure	37 kip (164.6 kN)	25 kip (111.2 kN)	42 kip (186.9 kN)
VRRSD prior to complete failure	0.46 in (11.7 mm)	0.44 in (11.2 mm)	0.34 in (8.6 mm)

4. Summary and conclusions

An FEA framework that incorporates concrete damage modeling and a unified bond model for pretensioned concrete crossties was employed to evaluate and compare the key performance of two common concrete tie designs, A and B. Tie A was made with eight prestressing strands, and Tie B was made with twenty prestressing wires. Four variations in the wire surface geometry were also included in the Tie B design to evaluate the effect of steel-concrete bond on the concrete tie performance. The FEA with the bond model demonstrated that the reinforcement properties including the surface geometry were key to differentiating concrete tie behaviors such as pretension-released surface strain profiles and splitting/bursting propensity but less influential on the flexural performance.

The flexural performance was evaluated in terms of load and vertical relative rail seat displacement (VRRSD) characteristics corresponding to the occurrence of AREMA-defined structural cracking and at complete tie failure. There appeared to be no significant differences in the performance of the five ties in the rail seat positive bending mode other than differences possibly introduced by the numerical method. All five ties satisfied (and likely exceeded) the AREMA concrete tie design criterion in the rail seat positive bending mode.

The center negative flexural performance was previously studied in a derailment investigation involving the Tie A design, and the study was extended to the Tie B design in this study. Both “no worn" (full pretension and full cross sections) and worn conditions (prestress loss and/or bottom abrasion) were considered for the concrete ties, along with a hypothetical deteriorated ballast support condition leading to center negative bending in the ties. The FEA conducted under the concrete tie "no worn" condition showed comparable load capacities of all five ties at structural cracking and complete failure, but the Tie A design displayed larger VRRSD capacities than the ties following the Tie B design. The FEA incorporating worn concrete tie conditions further concluded that the failure load capacity can be significantly reduced when prestress loss was combined with severe bottom abrasion in the concrete tie, potentially leading to unsafe track conditions with broken ties.

The FEA framework has demonstrated to be an effective tool for evaluating and comparing different concrete tie designs against key industrial performance and track safety requirements. It has shown full potential to be a cost-effective computational tool for optimizing the design of pretensioned concrete crossties.

5. References

1. American Railway Engineering and Maintenance-of-Way Association, Manual for Railway Engineering, Chapter 30, Part 4: Concrete Ties, 2010.
2. Arnold M. L., "Un-Tensioned Pullout Tests to Predict the Bond Quality of Different Prestressing Reinforcements Used in Concrete Railroad Ties," Doctoral dissertation, Kansas State University, 2013.
3. Bodapati, N. N. B., R. J. Peterman, W. Zhao, B. T. Beck, C. H. J. Wu, J. R. Holste, M. L. Arnold, R. Benteman, and R. Schweiger, "Transfer-Length Measurements on Concrete Railroad Ties Fabricated with 15 Different Prestressing Reinforcements," Proc. 2013 PCI Convention and National Bridge Conference, 2013.
4. Chen, Z., M. Shin, S. Wei, B. Andrawes, and D. A. Kuchma, "Finite Element Modeling and Validation of the Fastening Systems and Concrete Sleepers Used in North America," Proceedings of the Institution of Mechanical Engineers, Part F: Journal of Rail and Rapid Transit, Vol. 228, No. 6, 2014, pp. 590-602.
5. Choros, J., B. Marquis, and M. Coltman, "Prevention of Derailments Due to Concrete Tie Rail Seat Deterioration," Proceedings of the ASME/IEEE Joint Rail Conference and the ASME Internal Combustion Engine Division, Spring Technical Conference, 2007, pp. 173-181.
6. Dassault Systèmes Simulia Corp., Abaqus Analysis User's Manual, Version 6.12, Providence, RI, 2012.
7. Hanna, A. N., "State-of-the-Art Report on Prestressed Concrete Ties for North American Railroads," PCI Journal, September-October, 1979, pp. 32-61.
8. Lutch, R. H., Capacity Optimization of a Prestressed Concrete Railroad Tie, Master's Thesis, Michigan Technological University, 2009a.
9. Lutch, R. H., D. K. Harris, and T. M. Ahlborn, "Prestressed Concrete Ties in North America," AREMA Conference, 2009b.

10. Marquis, B. P., M. Muhlanger, and D. Y. Jeong, "Effect of Wheel/Rail Loads on Concrete Tie Stresses and Rail Rollover," Proceedings of the ASME 2011 Rail Transportation Division Fall Technical Conference, Minneapolis, MN, 2011.

11. Marquis, B. P., J. LeBlanc, H. Yu, and D. Y. Jeong, "CSX Derailment on Metro-North Tracks in Bronx, NY, July 18, 2013," Report to National Transportation Safety Board, United States, 2014, http://dms.ntsb.gov/pubdms/search/document.cfm?docid=417234&docketid=55312&mkey=87518

12. Mayville, R. A., L. Jiang, and M. Sherman, "Performance Evaluation of Concrete Railroad Ties on the Northeast Corridor," DOT/FRA/RPD-14/03. FRA, U.S. Department of Transportation, 2014.

13. Naaman, A. E., Prestressed Concrete Analysis and Design: Fundamentals, Third Edition, Techno Press 3000, 2012.

14. National Transportation Safety Board, "Railroad Accident Brief. NTSB/RAB-06/03," 2006.

15. National Transportation Safety Board, "Railroad accident brief – Metro-North Railroad derailment," Report no. NTSB/RAB-14/11, 2014.

16. Yu, H., D. Y. Jeong, J. Choros, and T. Sussmann, "Finite Element Modeling of Prestressed Concrete Crossties with Ballast and Subgrade Support," Proceedings of the ASME 2011 International Design Engineering Technical Conferences & Computers and Information in Engineering Conference, DETC2011-47452, 2011.

17. Yu, H., and D. Y. Jeong, "Railroad Tie Responses to Directly Applied Rail Seat Loading in Ballasted Tracks: A Computational Study," Proceedings of the ASME/ASCE/IEEE 2012 Joint Rail Conference, Philadelphia, Pennsylvania, 2012.

18. Yu, H., and D. Y. Jeong, "Bond between Smooth Prestressing Wires and Concrete: Finite Element Model and Transfer Length Analysis for Pretensioned Concrete Crossties," Proceedings of the 2014 ASCE Structures Congress, Boston, Massachusetts, 2014.

19. Yu, H., D. Jeong, B. Marquis, and M. Coltman, "Railroad Concrete Tie Failure Modes and Research Needs," Transportation Research Board 94th Annual Meeting, No. 15-0311, 2015a.

20. Yu, H., and D.Y. Jeong, "Finite Element Bond Models for Seven-Wire Prestressing Strands in Concrete Crossties," Proceedings of the ASME 2015 Joint Rail Conference, No. JRC2015-5758, 2015b.

21. Yu, H., "Estimating Deterioration in the Concrete Tie-Ballast Interface Based on Vertical Tie Deflection Profile: A Numerical Study," Proceedings of the ASME 2016 Joint Rail Conference, No. JRC2016-5783, 2016a.

22. Yu, H., and D.Y. Jeong, "Finite Element Bond Modeling for Indented Wires in Pretensioned Concrete Crossties," Proceedings of the ASME 2016 Joint Rail Conference, No. JRC2016-5782, 2016b.

23. Yu, H., B. P. Marquis, and D. Y. Jeong, "Failure Analysis of Railroad Concrete Crossties in the Center Negative Flexural Mode Using Finite Element Method," Proceedings of the Institution of Mechanical Engineers, Part F: Journal of Rail and Rapid Transit, Vol. 231, No. 5, 2017a, pp. 610-619.

24. Yu, H, "Finite Element Analysis of Contributing Factors to the Horizontal Splitting Cracks in Concrete Crossties Pretensioned with Seven-Wire Strands," Proceedings of the ASME 2017 Joint Rail Conference, No. JRC2017-2256, 2017b, https://ntl.bts.gov/lib/61000/61300/61352/JRC2017-2256-Yu.pdf

25. Yu, H., "Causes and Prevention of Splitting/Bursting Failure of Concrete Crossties: A Computational Study," American Railway Engineering and Maintenance-of-Way Association (AREMA) Annual Conference, Indianapolis, Indiana, United States, September 17-20, 2017c.

26. Yu, H., "A Unified Elastoplastic Bond Model for the Prestressing Steel Reinforcements Used in Railroad Concrete Crossties," In preparation for submission, 2018.

27. Zeman, J. C., J. R. Edwards, C. P. L. Barkan, and D. A. Lange, "Failure Mode and Effect Analysis of Concrete Ties in North America," Proc. of the 9th International Heavy Haul Conference, 2009, pp. 270-278.

28. Zhao, W., B. T. Beck, R. J. Peterman, C. H. J. Wu, G. Lee, and N. N. B. Bodapati, "Determining transfer length in pre-tensioned concrete railroad ties: is a new evaluation method needed?," Paper# RTDF2013-4727, Proceedings of the ASME 2013 Rail Transportation Division Fall Technical Conference, October 15-17, 2013, Altoona, PA.

6. Acknowledgment

The work described in this paper was sponsored by the Office of Research, Development and Technology, Federal Railroad Administration, U.S. Department of Transportation. Directions provided by Messrs. Gary Carr and Cameron Stuart of the Track Research Division are gratefully acknowledged. Daniel Mortarelli contributed to the work presented in this paper while employed as a Pathways Intern at the Volpe Center in the summer of 2016. Special thanks goes to Mr. Eric Wallischeck of the Center for Infrastructure Systems and Technology at the Volpe Center for his comprehensive comments that improved the quality of this paper.